

NJC

Accepted Manuscript



This is an *Accepted Manuscript*, which has been through the Royal Society of Chemistry peer review process and has been accepted for publication.

Accepted Manuscripts are published online shortly after acceptance, before technical editing, formatting and proof reading. Using this free service, authors can make their results available to the community, in citable form, before we publish the edited article. We will replace this *Accepted Manuscript* with the edited and formatted *Advance Article* as soon as it is available.

You can find more information about *Accepted Manuscripts* in the [Information for Authors](#).

Please note that technical editing may introduce minor changes to the text and/or graphics, which may alter content. The journal's standard [Terms & Conditions](#) and the [Ethical guidelines](#) still apply. In no event shall the Royal Society of Chemistry be held responsible for any errors or omissions in this *Accepted Manuscript* or any consequences arising from the use of any information it contains.

Viologen phosphorus dendritic molecule as carrier of ATP and Mant-ATP. Spectrofluorimetric and NMR studies.

Aleksandra Szulc^{a*}, Maria Zablocka^{b*}, Yannick Coppel^c, Christian Bijani^c, Wojciech Dabkowski^b, Maria Bryszewska^a, Barbara Klajnert-Maculewicz^a, Jean-Pierre Majoral^{c*}‡

^a Department of General Biophysics, University of Lodz, 141/143 Pomorska St., 90-236 Lodz, Poland..

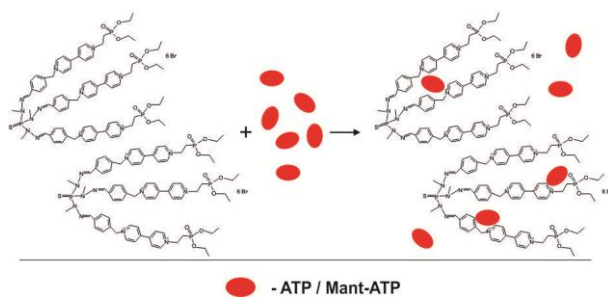
^b Centre of Molecular and Macromolecular Studies, Polish Academy of Sciences, Sienkiewicza 112, 90-363 Lodz, Poland.

^c Laboratoire de Chimie de Coordination du CNRS (LCC), 205 route de Narbonne, F-31077 Toulouse cedex 4, France.

majoral@lcc-toulouse.fr

* Authors contributed equally

‡ Corresponding author



A viologen phosphorus dendritic molecule is able to create non covalent interactions with model molecules of drugs belonging to nucleosides analogs.

ARTICLE

Viologen phosphorus dendritic molecule as carrier of ATP and Mant-ATP. Spectrofluorimetric and NMR studies.

Cite this: DOI: 10.1039/x0xx00000x

Received 00th January 2012,
Accepted 00th January 2012

DOI: 10.1039/x0xx00000x

www.rsc.org/

Aleksandra Szulc^{a*}, Maria Zablocka^{b*}, Yannick Coppel^c, Christian Bijani^c,
Wojciech Dabkowski^b, Maria Bryszewska^a, Barbara Klajnert-Maculewicz^a, Jean-
Pierre Majoral^{c‡}

In this work, the interactions between a viologen phosphorus dendrimer of generation 0 (VPD) and ATP or 2'-/3'-O-(N'-methylanthraniloyl)-ATP (Mant-ATP) were investigated by NMR and fluorescence spectroscopy methods. ATP and Mant-ATP were used as model molecules of purine and pyrimidine nucleoside analogs (NAs) which are antimetabolites commonly used in anticancer therapy. Complexes VPD with NAs may help to overcome of severe limitations of NAs associated with their low solubility, stability or resistance in cancer cells. The aim of the presented study was to evaluate stoichiometry and mechanism of forming complexes between dendrimers and nucleotides: ATP and Mant-ATP. Moreover, we examined the efficiency of complex formation in relation to temperature, a type of solvent, NaCl concentration, pH and environment polarity. It was observed that viologen phosphorus dendrimers create complexes with ATP and Mant-ATP with high efficiency. Obtained complexes are stabilized by electrostatic and aromatic-aromatic interactions as driving forces.

Keywords: viologen phosphorus dendrimers, nucleoside analogs, ATP, Mant-ATP, NMR, fluorescence spectroscopy, complexation.

Introduction

Drugs belonging to nucleoside analogs (NAs) are of widespread use in the treatment of cancer or as antiviral agents.¹⁻⁴ Fludarabine (9-β-D-arabinosyl-2-fluoroadenine F-ara-A) is one of the most common anticancer drug belonging to NAs group. F-ara-AMP is used in the treatment of hematological malignancies as B-cell chronic lymphocytic leukemia (B-CLL).⁵⁻⁷ Fludarabine is administered in a monophosphate form (F-ara-AMP) due to poor water solubility. However, immediately after intravenous administration F-ara-AMP is dephosphorylated to nucleoside form – F-ara-A.⁷⁻⁹ NAs are transported across biological membranes in the nucleoside form only. They require specialized nucleoside transporter (NT) proteins to cross through plasma membranes or be transported between intracellular compartments.^{3,10} Fludarabine influx is accomplished by hENT1 and hENT2 proteins.^{5,11} After entry into the cell fludarabine mechanism of action is the same as for other nucleoside analogues. It means that several phosphorylation reactions are required to design a toxic drug form. Only triphosphate form of fludarabine may exert cytotoxic effect against cancer cells. For this purpose, NAs are phosphorylated successively by deoxycytidine

kinase (dCK), monophosphate kinases (NMPK) and diphosphate kinases (NDPK) to 5'-mono-, di- and triphosphates. A reverse enzyme – 5'-nucleotidase (5'-NU) – is able to induce the dephosphorylation of active metabolites.^{8,11,12} A toxic effect of NAs is achieved by their interactions with nascent nucleic acids: DNA or RNA. The active form of NAs may interfere with intracellular enzymes, such as polymerases or ribonucleotide reductase, and modify the physiological nucleosides metabolism leading to apoptosis of cancer cells.^{4,13,14} Despite the high effectiveness of the NA drugs, therapy limitations associated with fast metabolism, low solubility, unfavorable biodistribution, cardiotoxicity, low specificity of interaction with the cancer cells or multidrug resistance are prevalent. Resistance of cancer cells may be associated with insufficient level of hENT or intracellular nucleoside kinases as well as with increased activity of 5'-nucleotidases or ribonucleotide reductase.^{1, 15-18} In order to overcome numerous therapy limitations including resistance mechanisms and to improve therapeutic effect of nucleoside analogs, several devices have been developed such as liposomes, linear polymers or dendrimers.¹⁹⁻²² Attaching of triphosphate form of nucleoside analogs to carriers such as dendrimers may help to overcome the resistance

mechanisms by delivering active metabolites directly into cancer cells independently on hENT proteins or intracellular enzymatic activation.

Dendrimers are a versatile class of polymers with well-defined monodispersed structure. Their unique structure with densely packed groups, modifiable multivalent surface and nanoscale size allows to apply them in pharmacy as drug delivery systems, in gene transfection or in imaging.²³⁻³⁰ Viologen phosphorus dendrimers (VPD) are a new class of dendrimers representing good candidates for nanocarriers of nucleoside analogs as fludarabine. VPDs are unique nanomolecules having both viologen (4,4'-bipyridinium) groups and phosphorus atoms in dendrimer branches.³¹⁻³³ 4,4'-bipyridinium salts also known as viologen groups are highly toxic. They are responsible for generation of reactive oxygen species and numerous damages of organs.^{34,35} Beside their significant toxicity, they present numerous promising application. Viologen dendrimers are able to complex small anionic guest molecules suggesting their potential application as drug nanocarriers.³⁶ A ternary light responsive complex between methyl viologen polymer, azobenzene and cucurbit[8]uril also exhibit capability to drug encapsulation which makes them promising candidate for advanced material engineering.³⁷ Numerous studies have shown that viologen phosphorus dendrimers demonstrate antiviral activity against HIV, HSV or respiratory syncytial viruses.^{38,39} Moreover, VPD as phosphorus dendrimers may prevent neurodegenerative processes *in vitro*.^{40,41}

Necessary features of the drug carriers are low toxicity and lack of immunogenicity.^{30,42} Dendrimer toxicity depends strongly upon the nature of the surface groups or molecular mass.^{42,43} Dendrimers with cationic groups on the surface are much more cytotoxic and hemolytic than anionic or neutral analogs, which results from the binding of cationic dendrimers to negatively charged cell membranes.^{15,44,45} Ciepluch *et al.* have proved that VPDs with phosphonate end groups are more hematotoxic than dendrimers possessing aldehyde end groups.⁴⁶ Surface modification with various neutral molecules such as polyethylene glycol (PEG), oligosaccharides, fatty acids or acetyl and glycidol groups allows to decrease dendrimer toxicity.^{15,45,47-49} The studies of biological features of VPD carried out by Ciepluch *et al.* and Lazniewska *et al.* have demonstrated promising outcomes for further applications of VPD as drug delivery devices.^{46,50} They have proved that VPD exert high toxicity against cancerous cell lines – N2a (mouse neuroblastoma cell line), while in contrast the control cell line B14 (Chinese hamster peritoneal fibroblasts cell line) was slightly sensitive to the used dendrimers.^{46,50}

In this paper we have examined the interactions between nucleotides and a viologen phosphorus dendrimer built from a trifunctionalized core P(S)(NCH₃NH₂)₃ and decorated on its surface with phosphonate groups (Fig. 1). We used ATP or 2'-/3'-O-(N'-methylanthraniloyl)-ATP (Mant-ATP) as model molecules (Fig. 2).

Materials and methods

Materials

Adenosine triphosphate (ATP) was purchased from Sigma Aldrich (Poland). 2'- / 3'-O-(N'-Methylanthraniloyl)-ATP (Mant-ATP) was purchased from Jena Bioscience

(Germany). The viologen phosphorus dendrimer (VPD) (MW 1890.13 g/mol) has been used and was synthesized in the Laboratoire de Chimie de Coordination du CNRS (LCC), Toulouse, France. Dendrimer chemical structure is presented in Figure 1. For fluorescent measurements MilliQ water, phosphate-buffered saline (PBS: 10mmol/L, pH 7.4, 137 mmol/L NaCl, 2.7 mmol/L KCl) phosphate buffer (10mmol/L, pH 6.0, pH 7.4 and pH 8.0), NaCl solution (50 mmol/L, 100 mmol/L and 137 mmol/L) and DMSO were used. For NMR measurements D₂O was used. Water used to prepare solutions was double-distilled.

NMR experiments

A stock solution of 1.2 mmol/L dendrimer sample was prepared by dissolving 10 mg of dendrimer in 4.2 mL of D₂O. This solution was separated in 7 identical samples where ATP was added to the dendrimer in order to obtain ATP concentrations of 1.2, 2.4, 4.8, 7.2, 9.6 and 12 mmol/L. All spectra were recorded on a Bruker Avance 500 spectrometer equipped with a 5 mm triple resonance inverse Z-gradient probe (TBI ¹H, ³¹P, BB). All chemical shifts for ¹H and ¹³C are relative to TMS using ¹H (residual) or ¹³C chemical shifts of the solvent as a secondary standard. The ROESY experiment was acquired with a mixing time of 300 ms. DOSY was used to measure the translational diffusion coefficient *D*. The DOSY spectra were acquired at 293K without temperature regulation in order to limit any convection phenomena. Measurements were performed with a diffusion delay Δ of 140 ms and a gradient pulse length δ of 2.2 ms for ATP alone, a Δ of 160 ms and a δ of 2.8 ms for dendrimer and dendrimer –ATP complex. The peak-integration decay curves of the DOSY spectra were fitted according to the Stejskal–Tanner function.⁵¹

Fluorescence titration experiments

The aim of our work was to evaluate the stoichiometry of interaction between viologen phosphorus dendrimer (VPD) and Mant-ATP (2'-/3'-O-(N'-methylanthraniloyl)-ATP). Additionally, efficiency of forming dendrimer – Mant-ATP complexes depending on (1) temperature (288 K, 298 K, 301 K, 308 K); (2) a type of solvent (water, PBS, phosphate buffer pH 7.4); (3) NaCl concentration (50 mmol/L, 100 mmol/L and 137 mmol/L); (4) pH (pH 6.0, pH 7.4, pH 8.0) and (5) polarity of environment (water, DMSO) was estimated.

Mant-ATP was used as a model molecule. The fluorescence intensity of Mant-ATP markedly depends on solvents or upon binding to most proteins making it an ideal molecule to study the binding efficiency of anticancer drugs belonging to the group of nucleoside analogues^{19,52} (Fig. 6). The solution of 1.5 μ mol/L ligand - Mant-ATP was titrated by the solution of binding agent – VPD. Fluorescence spectra were taken with a Jasco V-6300 spectrofluorometer. The excitation wavelength was set at 355 nm. The emission spectra were recorded from 400 to 500 nm and then fluorescence intensity was read at $\lambda_{\text{max}} = 445\text{nm}$. Each obtained spectrum was the average of three scans. Dendrimers were not excited by 355 nm wavelength and did not emit fluorescence in this range. Samples were contained in 1-cm path length quartz cuvettes and were continuously stirred and thermostated at appropriate temperature. The excitation and emission slit widths were set to 10 and 5 nm, respectively. Afterwards, changes in the fluorescence

intensity (F_{max}) and maximum fluorescence wavelength of Mant-ATP were recorded.

Table 1. ^1H NMR data assignments of dendrimer and ATP compounds in D₂O at 293K. (σ in ppm, J in Hz).

^1H atom	σ ^1H (n, mult, J)	
	dendrimer	ATP
1	3.28 (3H, d, 8.9)	6.03 (1H, d, 5.4)
2	7.92 (1H, s)	4.64 (1H, t, 5.2)
3	7.72 (2H, d, 8.4)	4.47 (1H, t, 4.4)
4	7.45 (2H, d, 8.4)	4.32 (1H, q, 2.9)
5	5.89 (2H, s)	8.52 (1H, s)
6	9.06 (2H, d, 6.8)	8.31 (1H, s)
7	8.46 (2H, d, 7.1)	4.20 (2H, m)
8	8.50 (2H, d, 6.6)	-
9	9.10 (2H, d, 6.8)	-
10	4.99 (2H, td, 7.3Hz ; 16.6)	-
11	2.77 (2H, td, 7.3Hz ; 18.3)	-
12	4.09 (4H, q, 7.1)	-
13	1.21 (6H, 7.14)	-

Results

NMR data analysis

Determination of the dissociation constant for the dendrimer – ATP interaction was achieved by fitting equation 1 to the chemical shift data obtained from the dendrimer – ATP titrations. Equation 1 is described for a multisite interaction of a guest (ATP) on the host (dendrimer).⁵³

$$A_{obs} = \frac{1}{2} A_{Max} \left[\left(1 + \frac{K_d}{n[P_0]} + \frac{[T_i]}{n[P_0]} \right) - \left\{ \left(1 + \frac{K_d}{n[P_0]} + \frac{[T_i]}{n[P_0]} \right)^2 - 4 \frac{[T_i]}{n[P_0]} \right\}^{\frac{1}{2}} \right] \quad (1)$$

Where A_{obs} is the chemical shift variation (ppm), K_d is the dissociation constant, n is the number of ATP per dendrimer, $[P_0]$ is the total concentration of dendrimer at each titration increment, and $[T_i]$ is the concentration of self-associated ATP. A_{Max} is the chemical shift difference between the chemical shifts of the dendrimer alone and saturated with ATP.

Chemical shift titration

^1H NMR titration has proved to be an effective tool in the analysis of interaction between dendrimers and guests.^{54,55} The ^1H signal of dendrimer and ATP compounds were

assigned (Tab. 1) on the basis of chemical shifts (δ), spin-spin coupling constants (J), splitting patterns and signal intensities, and by using ^1H - ^1H ROESY experiment.

The structure and ^1H numbering of the dendrimer and ATP is represented in Figure 1.

The dendrimer – ATP association was monitored by following the ^1H chemical shift variations of the dendrimer when ATP is added to the dendrimer (concentration constant all along the titration) at different concentrations (Fig. 2)

During the dendrimer – ATP titration, many of the proton signals of the dendrimer, particularly the $\text{CH}_3\text{-N}$ (H1-D, 3.28 ppm), the $\text{CH}=\text{N}$ (H2-D, 7.92 ppm), the H3-D (7.72 ppm) and H4-D (7.45 ppm) of the phenyl group and the CH_2 (H5-D, 5.89 ppm), were observed to shift at lower frequency (Fig. 2, S1, S2 and Tab. S1).

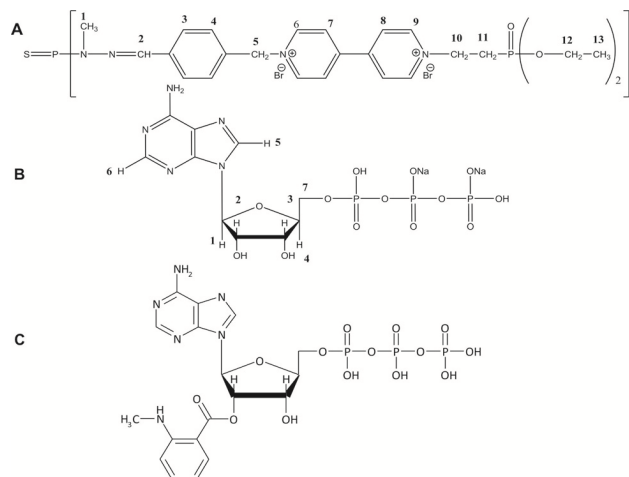


Figure 1. Chemical structures and hydrogen labeling in the viologen phosphorus dendrimer (A), ATP (B) and a chemical structure of Mant-ATP (C).

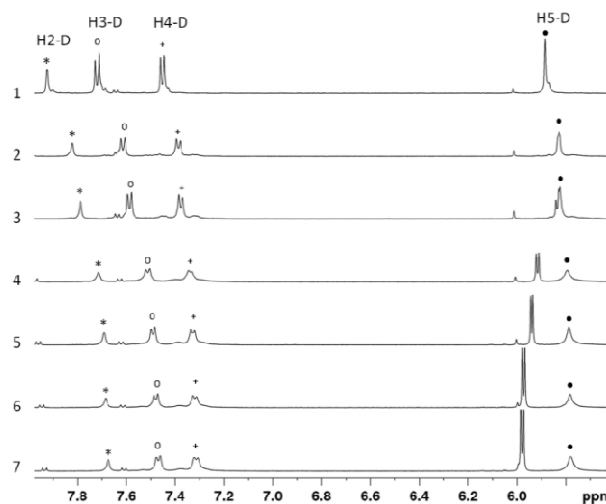


Figure 2. Expanded aromatic region of the ^1H NMR titration spectra of the dendrimer when mixed with ATP. The concentration of the dendrimer was kept constant at 1.2 mmol/L. The molar ratio of ATP – dendrimer ranges from 0 to 10 (1-7).

Dissociation constant for the ATP – dendrimer interactions and the number of molecule of ATP per dendrimer present on the dendrimer were obtained by fitting Eq.1 to the $\Delta\delta$ vs [ATP] binding curves (Fig. 3).

Dissociation constant (K_d) and number of ATP per dendrimer (n) were estimated by fitting Eq.1 to the dendrimer chemical shift data of H1-D and H11-D during the dendrimer – ATP titration. A K_d of $5.5 (\pm 0.3) \times 10^{-4}$ mol/L and a n value of 1.5 ± 0.1 ATP molecules per dendrimer were obtained. This correspond to an association constant ($K_a = 1/K_d$) of $1.8 (\pm 0.1) \times 10^3$ L/mol.

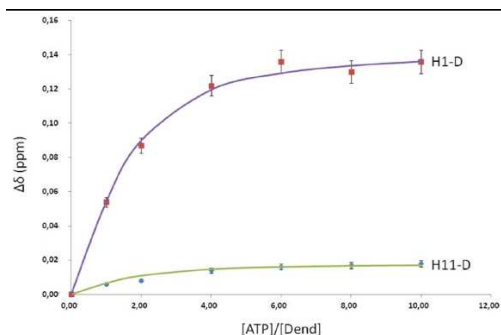


Figure 3. Comparison of the observed (symbols) and fitted (using Eq.1) chemical shift differences of the H1-D and H11-D dendrimer resonance with increasing ATP concentration

³¹P-NMR

³¹P NMR experiment of the dendrimer and ATP alone and of a 1/4 dendrimer – ATP mixture was acquired. Two ³¹P signals showed a significant shift: the one of the phosphorous in the core of the dendrimer with a shift at lower frequency of -28 Hz (left panel, Fig. 4A) and the one of the central phosphorous of ATP with a shift at higher frequency of 13 Hz (right panel, Fig. 4B).

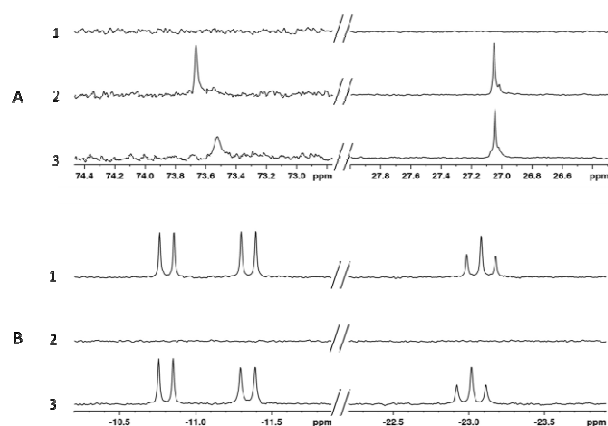


Figure 4. ³¹P NMR spectral signals for ATP (1) and the dendrimer (2) alone and for a 1/4 dendrimer – ATP mixture (3). The ³¹P NMR spectra of the dendrimer part are represented in A and of the ATP in B.

DOSY experiment

The hydrodynamic property of the dendrimer – ATP complex was studied by performing ¹H diffusion-ordered spectroscopy (DOSY) experiments. Decreases of the ATP and dendrimer diffusion coefficient D were observed in the 1/4 dendrimer – ATP mixture ($2.0 (\pm 0.1) \times 10^{-10} \text{ m}^2\text{s}^{-1}$ and $1.3 (\pm 0.1) \times 10^{-10} \text{ m}^2\text{s}^{-1}$ for ATP and the dendrimer, respectively) compared to the ones of ATP ($3.1 (\pm 0.2) \times 10^{-10} \text{ m}^2\text{s}^{-1}$) and dendrimer ($1.7 (\pm 0.1) \times 10^{-10} \text{ m}^2\text{s}^{-1}$) alone. This is in agreement with the formation of the dendrimer – ATP complex and with the presence of a fast exchange between bound and free molecules in the NMR diffusion timescale. Indeed, the observed coefficient diffusions for ATP and the dendrimer in the mixture (D_{obs}) are a weighted average of the free molecule (D_{free}) and of the ATP – dendrimer complexes diffusion coefficients ($D_{complexes}$): $D_{obs} = xD_{complexes} + (1 - x)D_{free}$ with a slower diffusion coefficient for the complex due to its bigger size.

ROESY experiment

2D-ROESY is a technique that provides information on the distance between protons in close spatial proximity within a given molecule, which is also used to detect host-guest interactions in complexes. In the spectrum, a cross-peak is only observed if the distance between the protons is less than 5 Å. ROESY spectra acquired from the molar ratio dendrimer – ATP: 1/4 was analyzed for the presence of intermolecular ROEs between protons of the dendrimer and protons of the ATP. Intermolecular ROEs were observed between the protons H3-D and H4-D of the dendrimer phenyl group and the protons H6-A and H5-A of the adenine and H1-A of the ribose ATP molecule (Fig. 5 and Fig. S4).

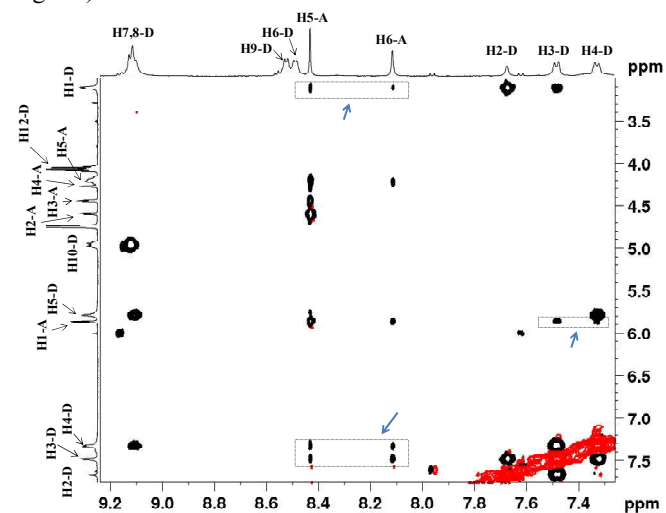


Figure 5. Aromatic region of the ¹H-¹H ROESY spectrum for dendrimer – ATP complex. Cross peaks shown in the rectangles indicate the through-space intermolecular correlation between the dendrimer and ATP.

Fluorescent titration data analysis

The fluorescence yield of Mant-ATP is strongly dependent on environmental conditions. The fluorescence intensity changes significantly upon binding to most proteins.⁵² The decrease in the fluorescence intensity and the shift in the fluorescence maximum of Mant-ATP were observed upon addition of dendrimers (Fig. 6). Noticed changes mean the ability of viologen phosphorus dendrimers to create complexes with Mant-ATP. Thus, Stern-Volmer method was used for analysis of obtained data. The process of fluorescence quenching of protein may be divided to static or dynamic.⁵⁶⁻⁵⁸ Standard Stern-Volmer equation for the dynamic quenching has the form as follows⁵⁶⁻⁵⁸:

$$\frac{F_0}{F} = 1 + K_{SV} [Q] \quad (2)$$

where F_0 and F are the fluorescence intensity in the absence and presence of quencher, respectively, K_{SV} is the Stern-Volmer constant and $[Q]$ is the concentration of quencher.

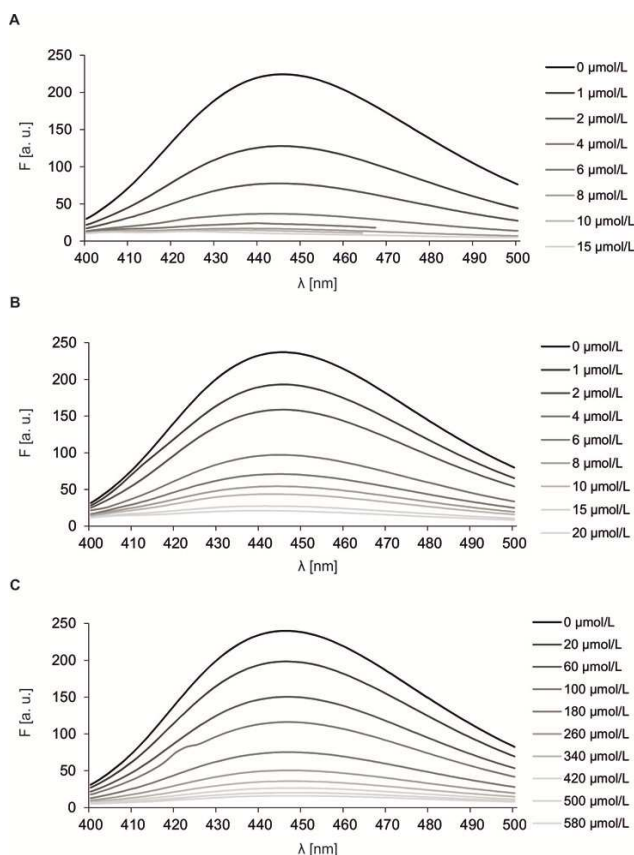


Figure 6. Fluorescence spectra of Mant-ATP after adding of VPD at increasing concentrations A – in water, B – in phosphate buffer pH 7.4, C – in PBS; $c_{\text{Mant-ATP}} = 1.5 \mu\text{mol/L}$, $\lambda_{\text{ex}} = 355 \text{ nm}$.

The obtained results have showed that not all of Stern-Volmer plots were linear, what may indicate that the static quenching mechanism is present in interaction between dendrimer and Mant-ATP.^{56,58} Typical Stern-Volmer equation for the static quenching takes the form⁵⁶⁻⁵⁸:

$$\frac{F_0}{F} = 1 + K_{SV} [Q] \exp(V[Q]) \quad (3)$$

where K_{SV} is the Stern-Volmer constant and V is the static quenching constant.

An additional way to distinguish of the quenching mechanism is examining the temperature dependence changes of quenching rate constant. At higher temperatures the static quenching is decreased while dynamic quenching is amplified.^{56,58} Thus, in order to verify the quenching mechanism, the fluorescence intensity of Mant-ATP upon increased concentration of dendrimers at different temperatures (288 K, 298 K, 301 K and 308 K) has been estimated. Mant ATP and dendrimer were dissolved in phosphate buffer (10 mmol/L, pH 7.4).

In the case of static quenching, the binding constant (K_b) and binding site number (n) for a quencher could be evaluated. Both parameters: K_b and n can be determined from a linear plot of $\log[(F_0-F)/F]$ on the ordinate versus $\log[Q]$ on the abscissa according to the equation⁵⁶⁻⁵⁸:

$$\log\left[\frac{F_0 - F}{F}\right] = \log K_b + n \log[Q] \quad (4)$$

where F_0 and F are the fluorescence intensity in the absence and presence of quencher, K_b is the binding constant, n is the number of binding sites and $[Q]$ is the concentration of quencher.

Figure 7A shows that the Stern-Volmer plots are linear and the slope decreases with higher temperature. Analysis of obtained graphs and Stern-Volmer constants presented in Table 2 clearly demonstrate that the quenching process is static.

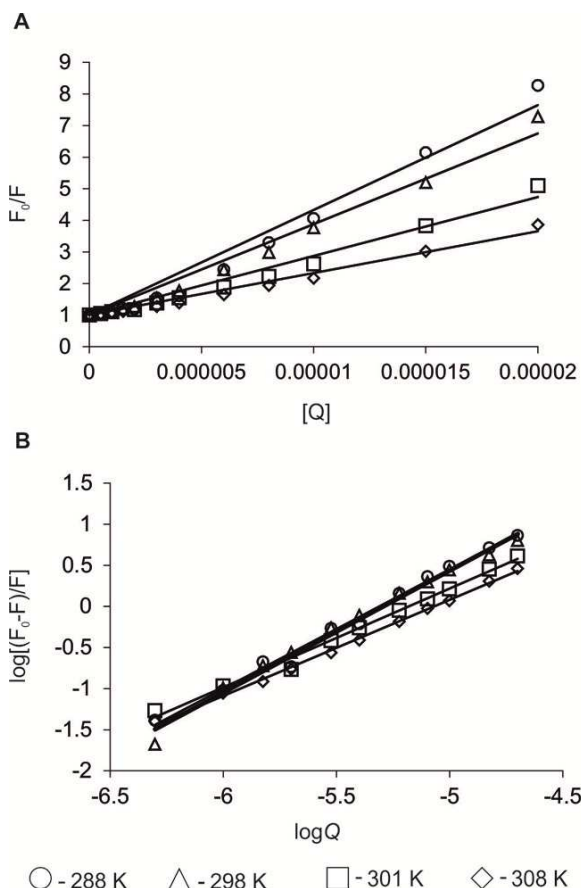
As shown in Figure 7B and Table 2, the number of binding sites and the binding constant decrease with increasing temperatures. However, the number of Mant-ATP molecules attached to the dendrimer does not differ significantly at different temperatures and is approximately equal to 1.

Table 2. Stern-Volmer constants (K_{SV}/V), binding constant (K_b), number of binding centers (n) and correlation coefficients for binding between Mant-ATP and VPD at various temperatures.

Temperature [K]	K_{SV} [L/mol]	r	V [L/mol]	r	n	K_b [L/mol]	r
288	$3.32 \cdot 10^5$	0.9663	-	-	1.45	$5.15 \cdot 10^7$	0.9906
298	$2.87 \cdot 10^5$	0.9782	-	-	1.48	$7.10 \cdot 10^7$	0.9886
301	$1.87 \cdot 10^5$	0.9748	-	-	1.20	$1.65 \cdot 10^6$	0.9915
308	$1.33 \cdot 10^5$	0.9819	-	-	1.17	$8.24 \cdot 10^5$	0.9979

The other variants of experiment have been carried out at 301 K, wherein the formation of complexes dendrimer – Mant-ATP was enough efficient and values of n and K_b were equal 1.20 and $1.65 \cdot 10^6 \text{ L/mol}$, respectively.

As it can be seen from Figure 6, complexes between viologen phosphorus dendrimers and Mant-ATP may be formed easily and the efficiency of complex formation depends on the reaction environment. Additional confirmation of noticed relationships are the values of n and



○ - 288 K △ - 298 K □ - 301 K ◇ - 308 K
Figure 7. Stern – Volmer plots for Mant-ATP fluorescence quenching by VPD at various temperatures (A); Plots of $\log[(F_0-F)/F]$ vs $\log Q$ (B); $c_{\text{Mant-ATP}} = 1.5 \mu\text{mol/L}$, $\lambda_{\text{ex}} = 355 \text{ nm}$.

K_b presented in the Table 3. The complex formation was the strongest in water, less marked in phosphate buffer (10 mmol/L; pH 7.4), and the weakest in PBS (10 mmol/L; 137 mmol/L NaCl, 2.7 mmol/L KCl, pH 7.4) (Tab. 3).

Besides, the maximum emission wavelength shift was monitored in order to study the environment of the Mant-ATP chromophore. A blue shift of the emission spectrum of Mant-ATP was observed after the addition of dendrimers in increasing concentrations but only in water and phosphate buffer, what is in good agreement with the conclusions drawn based on Stern-Volmer analysis (Tab. 3). Obtained results have indicated the location of Mant-ATP in more hydrophobic environment owing to Mant-ATP binding to the viologen phosphorus dendrimers.

The shift of λ_{max} and Stern-Volmer analysis have suggested that the efficient and rapid formation of complexes took place in water and phosphate buffer. It was evidenced by: rapid extinction of Mant-ATP fluorescence (Fig. 6; Fig. 8A), λ_{max} shift toward shorter wavelengths (Tab. 3) and the values of K_{SV} , V and K_b (Fig. 8A,C; Tab. 3). However, in PBS the weakest complex formation was observed, what may be caused by the presence of salt ions in PBS solution (137 mmol/L NaCl and 2.7 mmol/L KCl). In the case of experiment performed in PBS, λ_{max} shift was not observed (Tab. 3) and K_{SV} , V and K_b values were much lower than those for water and phosphate buffer (Fig. 8 B,C; Tab. 3). To confirm the supposition about the effects of salt ions to

form complexes, a further experiment using a solution of NaCl at different concentrations (50 mmol/L; 100 mmol/L and 137 mmol/L) was carried out.

The study of effectiveness of dendrimer – Mant-ATP complexes forming in NaCl solutions at different salt concentrations has proved that the content of salt ions in the solution influences on the capacity of Mant-ATP complexation with dendrimer. The first strong evidence was the size of the λ_{max} shift of fluorescence (Tab. 4).

The higher concentration of NaCl in the solution, the lower λ_{max} shift toward shorter wavelengths and the less efficient formation of complexes, appropriately (Tab. 4).

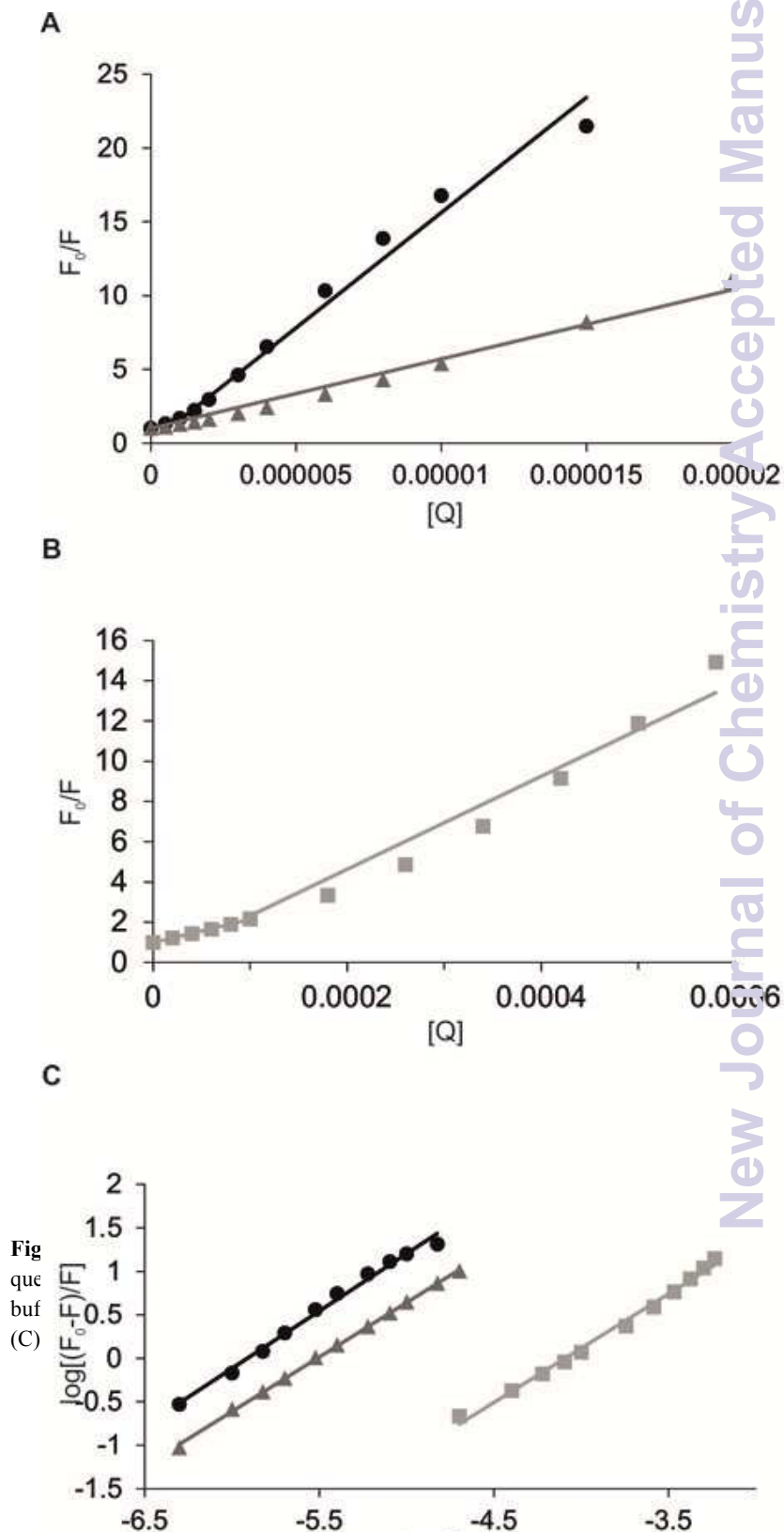


Fig 8
 que buf (C)

Furthermore, the most efficient fluorescence quenching of Mant-ATP upon addition of dendrimer has been observed in 50 mmol/L NaCl solution (Fig. 9A), what was also confirmed by the K_{SV} value derived from Stern-Volmer analysis (Tab.4). Taking into account the values of n and K_b parameters (Fig. 9B; Tab. 4) we may conclude that the number of Mant-ATP molecules attached to the dendrimer is not significantly different in each NaCl solution, however the salt molecules present in the PBS solution compete with Mant-ATP molecules for binding to dendrimer.

In the case of complexation of the nucleotide with the dendrimer in different pH phosphate buffer (6.0, 7.4 and 8.0), the most efficient Mant-ATP fluorescence quenching and the highest blue shift – 8 nm of the emission maximum were observed for the lowest pH – 6.0 (Fig. 10A; Tab.5). These results may be the consequence of the creation of strong electrostatic forces between dendrimer and Mant-ATP molecules. The values of K_b and n estimated from Figure 10B have indicated that pH of buffer has not such

significant influence on forming complexes between nucleotides and dendrimers.

Finally, the effect of the environment polarity to interaction between nucleotides and dendrimers has been compared. For this purpose two solvents having a different polarity: water and DMSO were used. The carried out experiment provides an evidence for efficient formation of complexes dendrimer – Mant-ATP. The DMSO solutions possess no ions which could affect or disrupt the complex formation. Therefore, we can be assured that the molecules of Mant-ATP interact directly with dendrimer molecules by forming stable complexes. In DMSO solution, fluorescence quenching of Mant-ATP by forming a complex with dendrimer has been observed after exceeding of 2 $\mu\text{mol/L}$ of dendrimer Mant-ATP (Fig. 11). Stern-Volmer analysis and the values of K_{SV} and K_b have indicated that the complexes are formed in both a polar (water) and a aprotic dipolar (DMSO) environment (Fig. 11, Tab. 6).

Table 3. Stern-Volmer constants (K_{SV}/V), binding constant (K_b), number of binding centers (n) and correlation coefficients for binding between Mant-ATP and VPD in various solvents; The maximum emission wavelength shift of Mant-ATP ($c = 1.5 \mu\text{mol/L}$) in the presence of VPD in various solvents ($\Delta\lambda$).

Reaction environment	K_{SV}		V		n	K_b		C_{KN155} [$\mu\text{mol/L}$]	$\Delta\lambda$
	[L/mol]	r	[L/mol]	r		[L/mol]	r		
Water	$7.48 \cdot 10^5$	0.9776	$2.00 \cdot 10^6$	0.9767	1.32	$6.34 \cdot 10^7$	0.9911	15	445nm \rightarrow 428nm
Phosphate buffer pH 7.4	$4.68 \cdot 10^5$	0.9857	-	-	1.25	$8.15 \cdot 10^6$	0.9992	20	445nm \rightarrow 440nm
PBS	$1.13 \cdot 10^4$	0.9971	$2.31 \cdot 10^4$	0.9546	1.25	$1.29 \cdot 10^5$	0.9926	580	-

Table 4. Stern-Volmer constants (K_{SV}/V), binding constant (K_b), number of binding centers (n) and correlation coefficients for binding between Mant-ATP and VPD in various NaCl concentrations; The maximum emission wavelength shift of Mant-ATP ($c = 1.5 \mu\text{mol/L}$) in the presence of VPD in various NaCl concentrations ($\Delta\lambda$).

C_{NaCl} [mmol/L]	K_{SV}		V		n	K_b		C_{KN155} [$\mu\text{mol/L}$]	$\Delta\lambda$
	[L/mol]	r	[L/mol]	r		[L/mol]	r		
50	$7.76 \cdot 10^4$	0.9969	-	-	1.12	$1.98 \cdot 10^5$	0.9962	580	445nm \rightarrow 443nm
100	$2.45 \cdot 10^4$	0.9950	$4.90 \cdot 10^4$	0.9701	1.28	$3.82 \cdot 10^5$	0.9969	580	445nm \rightarrow 447nm
137	$1.48 \cdot 10^4$	0.9924	$3.85 \cdot 10^4$	0.9485	1.39	$6.84 \cdot 10^5$	0.9949	580	445nm \rightarrow 448nm

Table 5. Stern-Volmer constants (K_{SV}/V), binding constant (K_b), number of binding centers (n) and correlation coefficients for binding between Mant-ATP and VPD in various pH; The maximum emission wavelength shift of Mant-ATP ($c = 1.5 \mu\text{mol/L}$) in the presence of VPD in various pH ($\Delta\lambda$).

pH	K_{SV}		V		n	K_b		C_{KN155} [$\mu\text{mol/L}$]	$\Delta\lambda$
	[L/mol]	r	[L/mol]	r		[L/mol]	r		
6.0	$6.19 \cdot 10^5$	0.9946	-	-	1.12	$2.49 \cdot 10^6$	0.9982	20	445nm \rightarrow 437nm
7.4	$4.68 \cdot 10^5$	0.9857	-	-	1.25	$8.15 \cdot 10^6$	0.9992	20	445nm \rightarrow 440nm
8.0	$2.83 \cdot 10^5$	0.9733	-	-	1.43	$3.74 \cdot 10^7$	0.9953	20	445nm \rightarrow 443nm

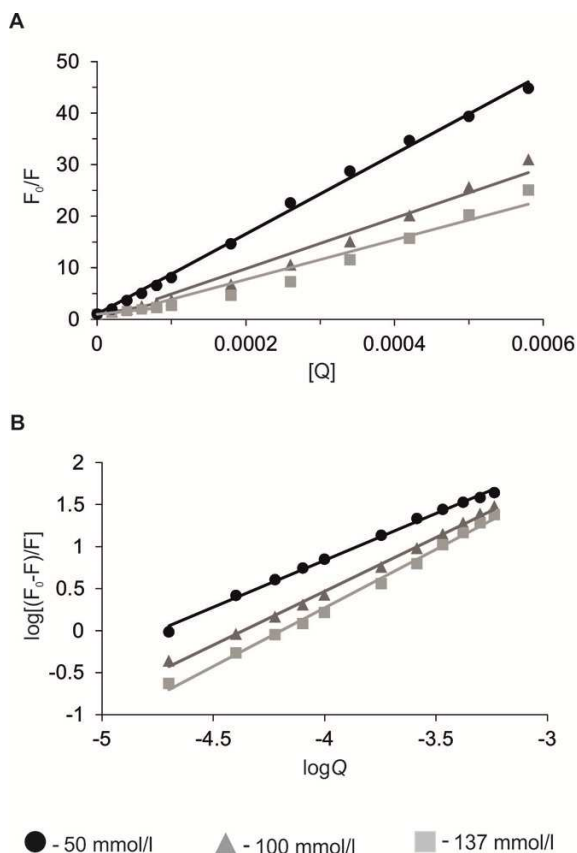


Figure 9. Stern – Volmer plots for Mant-ATP fluorescence quenching by VPD in various NaCl concentrations (A); Plots of $\log[(F_0-F)/F]$ vs $\log Q$ (B); $c_{\text{Mant-ATP}} = 1.5 \mu\text{mol/L}$, $\lambda_{\text{ex}} = 355 \text{ nm}$.

Table 6. Stern-Volmer constants (K_{SV}/V), binding constants (K_b), number of binding centers (n) and correlation coefficients for binding between Mant-ATP and VPD in water (polar solvent) or DMSO (aprotic dipolar solvent)

	K_{SV}		V		n	K_b	
	[L/mol]	r	[L/mol]	r		[L/mol]	r
Water	$7.48 \cdot 10^5$	0.9776	$2.00 \cdot 10^6$	0.9767	1.32	$6.34 \cdot 10^7$	0.9911
DMSO	$6.11 \cdot 10^4$	0.9348	-	-	1.53	$2.31 \cdot 10^7$	0.9775

Discussion

Recently, innovative solutions are extensively sought to increase the effectiveness of cancer therapies. The main obstacle is inefficient activity of anticancer drugs arising from various undesirable factors such as fast metabolism, unfavorable biodistribution, low specificity of interaction with the cancer cells or multidrug resistance. Although a plenty of fludarabine carriers have been investigated such as polymers or dendrimers¹⁹⁻²¹, new thriving strategies are still being looked for.

In the presented work, we have discovered that a new viologen phosphorus dendrimer may be a promising carriers of NAs such as fludarabine. The aim of this study was to

estimate the stoichiometry and characterization of the complexes formed between the viologen phosphorus dendrimer and model molecules of fludarabine: ATP and Mant-ATP. The results obtained by NMR studies have given us the first evidence for the formation of interactions between dendrimer and ATP. ^1H titration NMR experiment demonstrates that in the complex between the dendrimer and ATP, significant changes in chemical shifts of protons H1-D to H5-D of the dendrimer are observed. These proton chemical shift changes are localized in the interior of the dendrimer and provide evidence of interactions between the dendrimer and ATP.

This localization is confirmed by ROE cross-peaks between the dendrimer protons H1-D, H3-D and H4-D and the ATP protons H1-A, H5-A and H6-A that strongly suggest a π - π stacking interaction between the aromatic cycle of ATP and the phenyl groups located inside the dendrimer core. ROEs between protons 5 to 11 of the dendrimer and protons of the guest ATP cannot be observed, indicating that ATP compound is not localized in the periphery groups of the dendrimer. Furthermore, the ^{31}P chemical shift variations of the central phosphorus of ATP associated with ^1H chemical shift variations of the viologen protons (H6-D to H9-D) of the dendrimer (Figure 4 and S3) also indicate the presence of electrostatic interactions between the negatively charged ATP triphosphate and the positively charged dendrimer viologen groups³⁹.

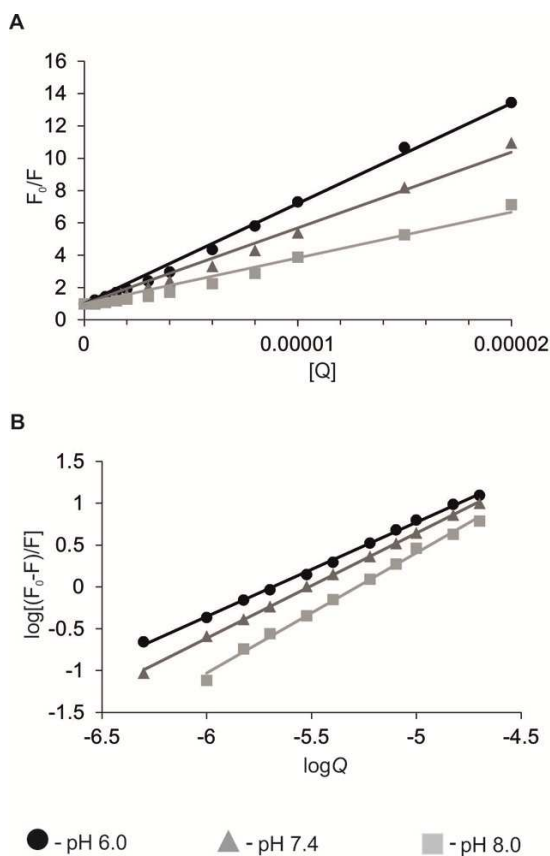


Figure 10. Stern – Volmer plots for Mant-ATP fluorescence quenching by VPD in various pH (A); Plots of $\log[(F_0-F)/F]$ vs $\log Q$ (B); $c_{\text{Mant-ATP}} = 1.5 \mu\text{mol/L}$, $\lambda_{\text{ex}} = 355 \text{ nm}$.

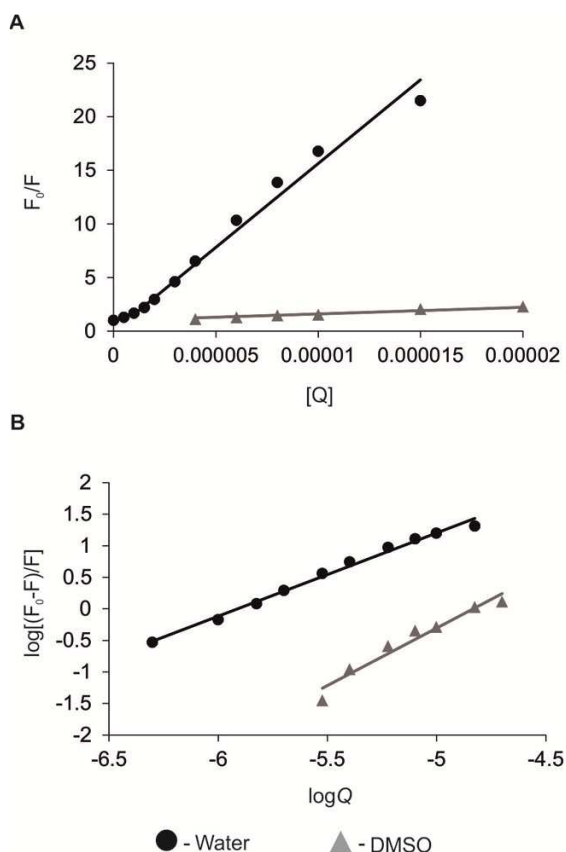


Figure 11. Stern – Volmer plots for Mant-ATP fluorescence quenching by VPD in various polarity environment (A); Plots of $\log[(F_0-F)/F]$ vs $\log Q$ (B); $c_{\text{Mant-ATP}} = 1.5 \mu\text{mol/L}$, $\lambda_{\text{ex}} = 355 \text{ nm}$.

An association constant of $1.8 (\pm 0.1) \times 10^3 \text{ L/mol}$ and a number of 1.5 ± 0.1 ATP molecules per dendrimer were calculated from the NMR titration. These results probably indicated the existence of two different types of complex in fast equilibrium with a dendrimer – ATP stoichiometry of 1:1 and 1:2 and in this case the K_a determined represent an average value for the two stoichiometries. This result also indicates that the binding of a third ATP molecule is unfavorable. Due to the location of the two ATP molecules in the core of the dendrimer, accessibility difficulties can be expected for the fixation of a third ATP molecule. DOSY experiments also confirm the complexation of the dendrimer with ATP molecules resulting in smaller diffusion coefficient for the two molecules. Unfortunately, the presence of fast exchange processes between the 1/1 and 1/2 dendrimer/ATP complexes and the free molecules resulting in observation of average diffusion coefficients:

$$D_{\text{obs}} = xD_{1-1-\text{Dendrimer:ATP}} + yD_{1/2-1-\text{Dendrimer:ATP}} + (1-x-y)D_{\text{free}}$$

do not allow to determine the hydrodynamic radius of the two different complexes. The presence of the dendrimer – ATP 1/2 adduct is definitively corroborated by mass spectrometry (figure S5) showing the presence of a set of signals centered at 1237.8 corresponding to a discharged dendriplex as well as by the presence of a set of signals at 1248.8 due to Na adduct. The results from the above mentioned analysis are in good accordance with the observations from a fluorescence

spectroscopy method. The characteristic of complexes of the dendrimer VPD with another fludarabine fluorescent derivative – Mant-ATP was determined. The shape of the Mant-ATP fluorimetric spectrum mightily depends upon its microenvironment. Ordinarily, the intensity of the fluorescence emission increased significantly after dendrimer or protein addition.^{19,52} When a PPI dendrimer of 5th generation was adding to Mant-ATP, the increase of Mant-ATP fluorescence was detected. Obtained result has proved that the complexes were formed between positive charged amino groups of the PPI dendrimer and negative charged phosphate groups of Mant-ATP. Upon the interaction of the dendrimer with nucleotide,¹⁹ an increase of Mant-ATP fluorescence was observed,¹⁹ whereas the complexation of VPD with Mant-ATP has shown a reverse outcome. The decrease in fluorescence may mean interactions of the dendrimer with an aromatic ring of Mant-ATP, which is located in the close vicinity of Mant-ATP chromophore. The π - π stacking interaction between aromatic cycle of Mant-ATP with groups located inside the dendrimer core hinders the conversion of the Mant-ATP chromophore and the increase in fluorescence. Thus, after binding all of the nucleotide molecules in the solution, a decrease of Mant-ATP fluorescence to minimum was observed (Fig. 6). Additional confirmation of the formation of VPD – Mant-ATP complexes is the shift in the position of the emission maximum. In general, the more effective the quench in fluorescence intensity observed, the more marked a blue-shift was recorded (Tab. 3).

Created VPD – Mant-ATP complexes are also stabilized by electrostatic interactions as proved by fluorescence spectroscopy. This was confirmed by the experiment carried out in phosphate buffers at various pH (6.0, 7.4 and 8.0). Lowering of the buffer pH might induce to generate –OH groups on the ATP instead of –ONa groups. According to the NMR studies, these –OH groups of ATP and specially the one on the central phosphorus of ATP form electrostatic interactions with the viologen protons (H6-D to H9-D) of the dendrimer. There is the strongest attraction of nucleotide in pH – 6.0 resulting in the most rapid decrease in fluorescence (Fig. 10) and the highest blue-shift of the emission maximum – 8 nm (Tab. 5).

All of tested variants of fluorescent experiments have shown that efficiency of forming VPD – Mant-ATP complexes depends on numerous factors such as a type of solvent, temperature, pH and other ions or molecules participating in the reaction. However, the observed changes were not so significant and in each tested case at least one nucleotide moiety was attached to the VPD dendrimer. An efficient complexation of nucleotide with dendrimer in a aprotic dipolar solvent – DMSO may also testify to high capability of VPD to forming stable complexes. The number of Mant-ATP molecules attached to the dendrimer and the binding constant for water and DMSO were equal $1.32 / 6.34 \times 10^7$ and $1.53 / 2.31 \times 10^7$, respectively.

It seems therefore that viologen phosphorus dendrimers are promising candidates for prospective application as drug vehicle. They may contribute to reduction of side effects connected with chemotherapy or overpassing of multidrug

resistance acquired during nucleoside analogs therapy.

Conclusions

In summary the ability of viologen phosphorus dendrimers to interact with nucleotides: ATP and Mant-ATP was investigated using NMR and fluorescence spectroscopy methods. The obtained results allowed us to formulate the following conclusions: (1) A cationic viologen phosphorus dendrimer is able to create stable complexes with negative charged nucleotides: ATP and Mant-ATP; (2) Dendrimer – ATP/Mant-ATP complexes are stabilized mainly by non-covalent electrostatic and aromatic-aromatic interactions; (3) Efficiency of forming complexes between dendrimer and ATP/Mant-ATP depends on various conditions such as type of solvent, pH, environment polarity, other ions or molecules participating in the reaction. Cationic viologen phosphorus dendrimers can be considered therefore as promising candidates for carriers of nucleoside analogs such fludarabine.

Acknowledgements

This work was partly supported by National Science Centre, Poland - Grant N N204 407740. This research was also funded by project “Biological Properties and Biomedical Applications of Dendrimers” operated within Foundation for Polish Science TEAM programme cofinanced by the European Regional Development Fund and by project „Dendrimers – potential drugs in chronic lymphocytic leukaemia” financed by National Science Centre, Poland

Notes and references

^a Department of General Biophysics, University of Lodz, 141/143 Pomorska St., 90-236 Lodz, Poland..

^b Centre of Molecular and Macromolecular Studies, Polish Academy of Sciences, Sienkiewicza 112, 90-363 Lodz, Poland.

^c Laboratoire de Chimie de Coordination du CNRS (LCC), 205 route de Narbonne, F-31077 Toulouse cedex 4, France.
majoral@lcc-toulouse.fr

- L. P. Jordheim, D. Durantel, F. Zoulim, Ch. Dumontet, *Nat. Rev. Drug Discov.*, 2013,12(6),447-464 [PubMed: 23722347].
- A. J. Berdis, *Biochemistry*, 2008,47(32),8253-8260 [PubMed: 18642851]
- M. Pastor-Anglada, P. Cano-Soldado, M. Molina-Arcas, M. P. Lostao, I. Larrayoz, J. Martinez-Picado and F. J. Casado, *Virus Res.*, 2005,107,151-164 [PubMed:15649561]
- C. M. Galmarini, J. R. Mackey and C. Dumontet, *Leukemia*, 2001,15,875–890 [PubMed: 11417472].
- F. Ricci, A. Tedeschi, E. Morra and M. Montillo, *Ther. Clin. Risk. Manag.*, 2009, 5,187–207 [PubMed: 19436622].
- E. L. Woodahl, J. Wang, S. Heimfeld, B. M. Sandmaier, P. V. O'Donnell, B. Phillips, L. Rislser, D. K. Blough and J. S. McCune, *Cancer Chemother. Pharmacol.*, 2009,63,391-401[PubMed: 18398611].
- T. Robak, *Transfus. Apher. Sci.*, 2005, 32, 33-44 [PubMed: 15737872].
- A. Janssens, M. Boogaerts and G. Verhoef, *Drug Des. Devel. Ther.*, 2009,3,241-52 [PubMed: 20054443].
- V. Gandhi and W. Plunkett, *Clin. Pharmacokinet.*, 2002,41,93-103 [PubMed: 11888330].
- J. Zhang, F. Visser, K. M. King, S. A. Baldwin, J. D. Young and C. E. Cass, *Cancer Metastasis Rev.*, 2007,26,85–110 [PubMed: 17345146].
- C. M. Galmarini, J. R. Mackey and Ch. Dumontet, *Lancet Oncol.*, 2002,3,415–424 [PubMed: 12142171].
- L. P. Jordheim and C. Dumontet, *Biochim. Biophys. Acta*, 2007,1776,138–159 [PubMed: 17881132].
- B. Ewald, D. Sampath and W. Plunkett, *Oncogene*, 2008,27,6522–6537 [PubMed: 18955977].
- C. M. Galmarini, G. Warren, E. Kohli, A. Zeman, A. Mitin and S. V. Vinogradov, *Mol. Cancer Ther.*, 2008,7,3373–3380 [PubMed: 18852140].
- P. Kesharwani, K. Jain and N. K. Jain, *Prog. Polym. Sci.*, 2014,39,268–307.
- Ch-M. J. Hu, S. Aryal and L. Zhang, *Ther. Deliv.*, 2010,1,323-334 [PubMed: 22816135].
- H. Hillaireau, T. Le Doan, and P. J. Couvreur, *J. Nanosci. Nanotechnol.*, 2006,6,2608-2617 [PubMed: 17048470].
- P. Menna, E. Salvatorelli and G. Minotti, *Chem. Res. Toxicol.*, 2008,21,978-989 [PubMed: 18376852].
- A. Szulc, D. Appelhans, B. Voit, M. Bryszewska and B. Klajnert, *J. Fluoresc.*, 2013,23,349-356 [PubMed: 23306952].
- N. Polikarpov, D. Appelhans, P. Welzel, A. Kaufmann, P. Dhanapal, C. Bellmann and B. Voit, *New J. Chem.*, 2012,36,438-451.
- S. V. Vinogradov, A. D. Zeman, E. V. Batrakova and A. V. Kabanov, *J. Control. Release*, 2005,107,143-157 [PubMed: 16039001].
- A. Hamada, T. Kawaguchi and M. Nakano, *Clin. Pharmacokinet.*, 2002,41,705-718 [PubMed: 12162758].
- S. Mignani, S. El Kazzouli, M. Bousmina and J.P. Majoral, *Chem. Rev.*, 2014,114(2),1327-1342
- S. Mignani and J.P. Majoral, *New. J. Chem.*, 2013,37(11),3337-3357
- A.M. Caminade and J.P. Majoral, *New J. Chem.*, 2013,37(11),3358-3373
- S. Mignani, S. El Kazzouli, M. Bousmina and J.P. Majoral, *Prog. Polym. Sci.*, 2013,38,993-1008
- S. Mignani, S. El Kazzouli, M. Bousmina and J.P. Majoral, *Adv. Drug Deliv. Rev.*, 2013,64,1316-1330
- E. Blattes, A. Vercellone, H. Eutamene, C.O. Turrin, V. Theodorou, J.P. Majoral, A.M. Caminade, J. Prandi, J. Nigou and G. Puzo, *Proceedings Nat. Acad. Sci. of the USA*, Early Edition 2013,(May 13, 2013)
- D. Astruc, E. Boisselier and C. Ornelas, *Chem. Rev.*, 2010,110,1857–1959 [PubMed: 20356105].
- B. K. Nanjwade, H. M. Bechraa, G. K. Derkara, F. V. Manvia and V. K. Nanjwade, *Eur. J. Pharm. Sci.*, 2009,38,185–196 [PubMed: 19646528].

- 31 N. Katir, J. P. Majoral, A. El Kadib, A. M. Caminade and M., Bousmina, *Eur. J. Org. Chem.*, 2012,269-273.
- 32 M. Kathiresan, L. Walder, F. Ye and H. Reuter, *Tetrahedron Lett.*, 2010,51,2188–2192.
- 33 P. Bhattacharya and A. E. Kaifer, *J. Org. Chem.*, 2008,73,5693-5698 [PubMed: 18598083].
- 34 T. Fukushima, K. Tanaka, H. Lim and M. Moriyama, *Environ. Health Prev. Med.*, 2002,7,89–94.
- 35 J. M. Moran, M. A. Ortiz-Ortiz, L. M. Ruiz-Mesa and J. M. Fuentes, *J. Biochem. Mol. Toxicol.*, 2010,24,402–409 [PubMed: 21182169].
- 36 M. Kathiresan and L. Walder, *Macromolecules*, 2011,44,8563-8574.
- 37 C. Stoffelen, J. Voskuhl, P. Jonkheijm and J. Huskens, *Angew. Chem. Int. Ed.*, 2014, 53,3400 –3404 [PubMed: 24615852].
- 38 S. Asaftei, D. Huskens and D. Schols, *J. Med. Chem.*, 2012,55(23),10405-10413 [PubMed: 23157587].
- 39 S. Asaftei and E. De Clercq, *J. Med. Chem.*, 2010,53,3480–3488 [PubMed: 20377249].
- 40 K. Milowska, J. Grochowina, N. Katir, A. El Kadib, J. P. Majoral, M. Bryszewska and T. Gabryelak, *J. Luminesc.*, 2013,134,132–137.
- 41 T. Wasiak, M. Ionov, K. Nieznanski, H. Nieznanska, O. Klementieva, M. Granell, J. Cladera, J. P. Majoral, A. M. Caminade and B. Klajnert, *Mol. Pharm.*, 2012,9,458–469 [PubMed: 22206488].
- 42 S. Svenson, *Eur. J. Pharm. Biopharm.*, 2009,71,445–462 [PubMed: 18976707].
- 43 B. Klajnert, J. Janiszewska, Z. Urbanczyk-Lipkowska, M. Bryszewska, D. Shcharbin and M. Labieniec, *Int. J. Pharm.*, 2006,309,208–217 [PubMed: 16386860].
- 44 B. Klajnert, S. Pikala and M. Bryszewska, *Proc. R. Soc. A*, 2010,466,1527–1534.
- 45 K. Jain, P. Kesharwani, U. Gupta and N. K. Jain, *Int. J. Pharm.*, 2010,394,122–142 [PubMed: 20433913].
- 46 K. Ciepluch, N. Katir, A. El Kadib, A. Felczak, K. Zawadzka, M. Weber, B. Klajnert, K. Lisowska, A. M. Caminade, M. Bousmina, M. Bryszewska, and J. P. Majoral, *Mol. Pharm.*, 2012,9,448–457 [PubMed: 22214284].
- 47 B. Klajnert, D. Appelhans, H. Komber, N. Morgner, S. Schwarz, S. Richter, B. Brutschy, M. Ionov, A. K. Tonkikh, M. Bryszewska and B. Voit, *Chemistry*, 2008,14,7030-7041 [PubMed: 18576443].
- 48 J. B. Wolinsky and M. W. Grinstaff, *Adv. Drug Deliv. Rev.*, 2008,60,1037-1055 [PubMed: 18448187].
- 49 S. Svenson and D. A. Tomalia, Dendrimers in biomedical applications-reflections on the field. *Adv. Drug Deliv. Rev.*, 2005;(57):2106-2129 [PubMed: 16305813].
- 50 J. Lazniewska, A. Janaszewska, K. Miłowska, A. M. Caminade, S. Mignani, N. Katir, A. El Kadib, M. Bryszewska, J. P. Majoral, T. Gabryelak and B. Klajnert-Maculewicz, *Molecules*, 2013,18,12222-12240 [PubMed: 24084024].
- 51 E. O. Stejskal and J. E. Tanner, *J. Chem. Phys.*, 1965,42,288–292.
- 52 A. Leskovar and J. Reinstein, *Arch. Biochem. Biophys.*, 2008,473,16–24 [PubMed: 18342617].
- 53 A. J. Charlton, N. J. Baxter, M. L. Khan, A. J. G. Moir, E. Haslam, A. P. Davies and M. P. Williamson, *J. Agric. Food Chem.*, 2002,50,1593–1601 [PubMed: 11879042].
- 54 Q. L. Wu, Y. Y. Cheng, J. J. Hu, L. B. Zhao and T. W. Xu, *J. Phys. Chem. B.*, 2009,39,12934-12943 [PubMed: 19775177].
- 55 K. Yang, Y. Y. Cheng, X. Y. Feng, J. H. Zhang, Q. L. Wu and T. W. Xu, *J. Phys. Chem. B.*, 2010,114,7265–7273 [PubMed: 20462223].
- 56 J. Li, J. Li, Y. Jiao and Ch. Dong, *Spectrochim. Acta A Mol. Biomol. Spectrosc.*, 2014,118,48-54 [PubMed: 24036307].
- 57 M. Ferenc, E. Pedziwiatr-Werbicka, K. E. Nowak, B. Klajnert, J. P. Majoral and M. Bryszewska, *Molecules*, 2013,18,4451-4466 [PubMed: 23591925].
- 58 H. Sun, Y. Wu, X. Xia, X. Liu and Z. Shi, *Chemical Monthly*, 2013,144,739-746.
- 59 .One can postulate that the pH could change with the dendrimer/ATP ratio. Given the chemical structure of the ATP and the dendrimer molecules, we can expect higher chemical shift changes following pH modification for the ATP than for the dendrimer molecules. Indeed, ^{31}P NMR shift of ATP is frequently used to determine intracellular pH. Of the three phosphorus ATP, it is the $\gamma\text{-P}$ that shows the highest ^{31}P NMR shift depending on the pH (up to 5 ppm), following by the $\beta\text{-P}$ (up to 1.5 ppm) and the $\alpha\text{-P}$ (up to 0.2 ppm)^{60,61}. In our case, we observed a ^{31}P chemical shift change of only +1.1 Hz (0.005 ppm) for the $\gamma\text{-P}$ of ATP from the sample of ATP alone versus the one of the 1/4 dendrimer-ATP mixture. The change was of + 13.0 Hz for the $\beta\text{-P}$ and of 1.0 Hz for the $\alpha\text{-P}$. This result indicates that the pH does not change notably for our dendrimer/ATP samples. Furthermore we have generally observed in previous studies that slight changes in pH values has no or very small effects on ^1H NMR chemical shifts of dendrimers without sites that can be engaged in acid-base equilibria. It seems reasonable to estimate than the ^1H chemical shift variation of protons located in the hydrophobic dendrimer core (used for the dissociation constant determination) is only due to the binding between dendrimer and ATP and is not affected by pH variations (at the error level).
- 60 T.D.Son, M. Roux, M. Ellenberger, *Nucl. Ac. Res.*, 1975, 2, 1101-1110.
- 61 A. V.Cherepanov, E.V. Doroshenko, J. Matysik, S. De Vries, H. J. M. De Groot, *Phys. Chem. Chem. Phys.*, 2008, 10, 6820-6828.